NASA TECHNICAL NOTE

NASA TN D-5414

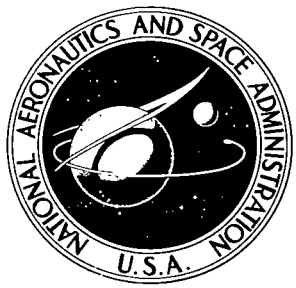

NASA TN D-5414

ANALYTICAL AND EXPERIMENTAL STUDIES OF MHD GENERATOR CATHODES EMITTING IN A "SPOT" MODE

by Lester D. Nichols and Maris A. Mantenieks

Lewis Research Center
Cleveland, Ohio

NATIONAL AERONAUTICS AND SPACE ADMINISTRATION • WASHINGTON, D. C. • SEPTEMBER 1969

ANALYTICAL AND EXPERIMENTAL STUDIES OF MHD GENERATOR CATHODES EMITTING IN A "SPOT" MODE

By Lester D. Nichols and Maris A. Mantenieks

Lewis Research Center
Cleveland, Ohio

NATIONAL AERONAUTICS AND SPACE ADMINISTRATION

For sale by the Clearinghouse for Federal Scientific and Technical Information
Springfield, Virginia 22151 – CFSTI price $3.00

ABSTRACT

The sheath current-voltage characteristics for a plane cathode emitting current from a thermionic arc spot are derived. The derivation is based upon the requirement of energy conservation at the cathode spot and also in an ionization region adjacent to the spot. The results for given gas conditions and electrode work function predict a sheath voltage which decreases with both increasing current for a fixed undisturbed (i. e., far from the spot) cathode temperature, and increasing undisturbed cathode temperature at a fixed current. Experimental data is shown which supports the conclusions predicted by the model.

ANALYTICAL AND EXPERIMENTAL STUDIES OF MHD GENERATOR CATHODES EMITTING IN A "SPOT" MODE

by Lester D. Nichols and Maris A. Mantenieks

Lewis Research Center

SUMMARY

A simple physical model for the behavior of thermionic arc spots on MHD generator cathodes is presented. In this model ions are accelerated through a sheath to the cathode by the cathode voltage drop. Both kinetic energy and ionization energy are transferred to the cathode. A spot forms whose size and temperature are determined from an energy balance between the heat transferred to the cathode by the ions (and possibly excited state atoms) and the heat transferred from the spot by conduction in the cathode.

It is assumed that the ions are created by electron collisions in the gas in a region near the cathode. The electrons are thermionically emitted from the cathode. They are accelerated from the cathode into this ionization region by the same cathode voltage drop which accelerates the ions to the cathode. An energy and mass balance in this ionization region along with the equation of state for a perfect gas can be used to determine the ion current.

Based upon the present model, the effects of varying the current, gas pressure, and undisturbed (i. e., far from the spot) cathode temperature are predicted. An increase in any one of these parameters (while holding the other two parameters constant) will result in a decrease in the cathode sheath voltage drop and an increase in the cathode spot temperature. The cathode spot size and heat transfer to the cathode spot increase with increasing current, but decrease with increasing pressure and undisturbed cathode temperature. This model can be used in MHD generator design to predict the effects of varying load current, gas pressure, and electrode temperature upon cathode spot parameters.

The electrical characteristics of 2 percent thoriated tungsten cathodes used in a supersonic MHD generator have been studied experimentally. The generator working fluid is pure argon which is arc heated. A single pair of electrodes is studied. The electrodes are flat plates held parallel to the flow direction and away from the generator wall. Illuminated spots are apparent on the cathode when current is flowing in the generator load circuit. At the same time a region of higher ion concentration in the argon near the spot is observed by spectroscopic measurements. The cathode voltage drop and temperature of the spot have been measured as a function of the arc spot current. The results of the experiment are in agreement with the predictions of the model.

INTRODUCTION

The mode of electron emission from an MHD generator cathode can affect the performance of the generator. Under certain conditions the emission of the electrons is confined to a small spot on the cathode. These spots are similar to the spots observed in any thermionic arc (ref. 1). There are many theoretical studies of these arc spots, and they have in common the assumption that the spot is formed by ion energy transfer to the cathode. The ions are formed in a region near the cathode as a result of electron collisions with gas atoms. The differences among the previous studies involve their treatment of the ionization region and the number of unknown parameters which must be specified in order to use the model to predict current voltage characteristics. Ecker (ref. 2) determines the ion current from the solution which gives the minimum voltage as a function of a "contraction parameter" rather than considering the energy conducted from the spot. Bauer (ref. 3) and Lee and Greenwood (ref. 4) leave the ion current as a free parameter to be determined experimentally. Adams and Robinson (ref. 5) consider a rather complete set of heat transfer mechanisms, but require the specification of the angle between the current stream tube and the normal to the cathode before comparison between their model and experiment can be made. The aim of this study is to present a model which requires no empirical constants. Such a theory is presented by Bade and Yos (ref. 6). But they make many assumptions about the nature of the phenomena to develop a simple theory. The present report is an attempt to improve the Bade and Yos theory by using fewer assumptions but retaining simplicity. Bade and Yos assume that the ions and electrons are at the same temperature, all the atoms are ionized, and that the electron current carries no energy from the ionization region into the discharge. We offer a means of calculating electron temperature, ion density, and the energy carried by the electrons from the ionization region to the discharge volume. In all other respects these two models are the same.

THEORETICAL MODEL

Cathode Energy Conservation

The electron current in a thermionic arc (i.e., an arc whose electron current can be accounted for by thermionic emission from the cathode) is supplied by thermionic emission from a spot of radius R on the cathode. The size of this spot can be estimated from an energy balance at the cathode surface. The energy impinging on the surface is assumed to come from an ion flux. This ion flux, in turn, is assumed to originate in an "ionization region" shown in figure 1. The ionization is accomplished as a result of the

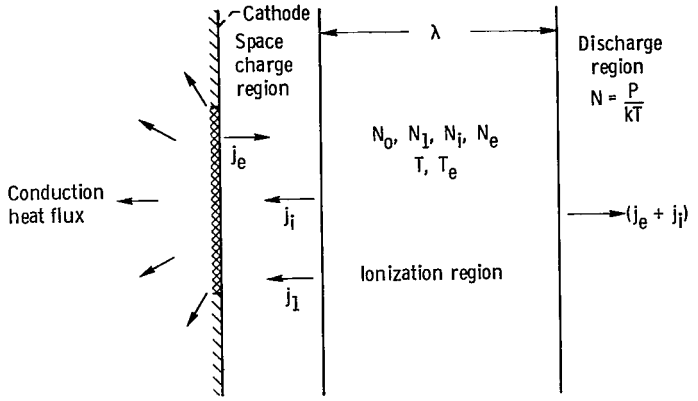

Assumed phenomenon	Space charge region	Ionization region	Discharge region
Collisions	None	Ionization, excitation, maxwellization	Elastic
Electron temperature	Not defined	$3/2\ kT_e = 1/2\ e(\varphi_{ion} - \varphi_1)$	Varying
Pressure; heavy temperature		Uniform	

Figure 1. - Sketch showing cathode spot, space charge region, ionization region, and discharge region. Also shown are descriptions of type of assumed phenomena occurring in each region.

acceleration of the electrons emitted from the spot. The energy transported by the ion flux is proportional to the ion current times the net potential energy of the ions (ref. 1):

$$j_i(V_{sh} + \varphi_i - \varphi_w)$$

This expression assumes neutralization of all ions at the cathode (no ion reflection), and all of the ion energy is transferred to the cathode (an accommodation coefficient of 1). There is also a flux of excited neutrals to the cathode. The energy transported by this flux is $j_1\varphi_1$. This expression assumes deexcitation at the cathode. The electron current emitted from the spot takes with it energy:

$$j_e\left(\varphi_w + 2\frac{k}{e}T_s\right)$$

Herein we will consider work functions such that the electrode spot temperature contribution can be neglected.

If the spot area is small compared to the electrode area, then the energy conducted from the spot is (ref. 9)

$$4RK(T_s - T_\infty)$$

If the cathode is in radiation equilibrium with its surroundings at zero current (i.e., with no spot), then the additional energy required to maintain the additional radiated energy because of the spot is

$$\pi R^2 \epsilon\sigma(T_s^4 - T_\infty^4)$$

If there is no mass transfer from the cathode, then the steady state energy balance must be

$$4RK(T_s - T_\infty) = \pi R^2\left[j_i(V_{sh} + \varphi_i - \varphi_w) + j_1\varphi_1 - j_e\varphi_w - \epsilon\sigma\left(T_s^4 - T_\infty^4\right)\right] \tag{1}$$

This equation provides a relation between the spot temperature, spot radius, and the various particle currents. The electron current can be related to the spot temperature by the Richardson equation

$$j_e = A_{rich}T_s^2 \exp - \left(\frac{e\varphi_w}{kT_s}\right) \tag{2}$$

The ion current can be related to the electron current if one considers a mass balance and equation of state in the ionization region.

Ionization Region

Mass conservation. - Assume that the ion current is given by the random thermal current:

$$j_i = \frac{1}{4} eN_i v_i \tag{3}$$

where

$$v_i = \sqrt{\frac{8kT_i}{\pi m_i}} \tag{4}$$

The ion temperature in the ionization region is assumed to be equal to the neutral temperature, and both are assumed to be the same in the ionization region as in the discharge region. The ion number density will, of course, be influenced by the electrons which are carried to the region. In order to calculate this quantity, an ionization model must be established. We will assume that the atoms have three energy levels: ground state, first excited state, and ionization. Also, we assume that the pressure in the ionization region is the same as in the remainder of the gas. This assumption will be accurate only when the pressure gradients required to provide the particle flux lead to small pressure changes in the ionization region. For this case, then

$$\frac{P}{kT} \equiv N = N_o + N_1 + N_i + \frac{T_e}{T} N_e \tag{5}$$

since the atoms and ions all have the same temperature. If one also assumes charge neutrality and defines the temperature ratio r as

$$r \equiv \frac{T_e}{T} \tag{6}$$

and the parameter p as

$$p \equiv \frac{N_o + N_1}{N_i} \tag{7}$$

then equation (5) can be written as

$$\frac{N_i}{N} = \frac{1}{1 + r + p} \tag{8}$$

To estimate the size of the parameter p, consider the continuity equations which determine the number density of the three levels of the model atom. A three level model atom oversimplifies the actual situation, but the results can be used to determine trends (ref. 7). The collision cross section for excitation from the ground state is Q_{o1}, and the collision cross section for ionization from the excited state is Q_{1i} and from the ground state is Q_{oi}. The continuity equations can be integrated over a planar ionization region of thickness λ (see fig. 1) and written as

$$j_i = \lambda e \left(\langle Q_{oi} v_e N_e \rangle N_o + \langle Q_{1i} v_e N_e \rangle N_1 \right) \tag{9}$$

$$j_1 = \lambda e \left(\langle Q_{o1} v_e N_e \rangle N_o - \langle Q_{1i} v_e N_e \rangle N_1 \right) \tag{10}$$

$$j_o = -\lambda e \left(\langle Q_{oi} v_e N_e \rangle + \langle Q_{o1} v_e N_e \rangle \right) N_o \tag{11}$$

The variables have been assumed to be constant in the ionization region and $\langle\ \rangle$ denotes an average over the electron energy distribution. These continuity equations imply no radiative deexcitation or recombination in the ionization region. This is a good assumption for the neutral pressures and electron temperatures considered in this study (refs. 7 and 10).

The probability of ionization from the excited state is larger than for the other two collisions considered, assuming that once an atom is excited to this state it will be ionized immediately, and that the flux of excited particles from the ionization region will be zero. This assumption is valid for a large ratio of electron current to flux of ground state atoms. Then, equation (10) implies

$$N_1 = \frac{\langle Q_{o1} v_e N_e \rangle}{\langle Q_{1i} v_e N_e \rangle} N_o \tag{12}$$

Equation (9) can now be written as

$$j_i = \lambda e N_o \left(\langle Q_{oi} v_e N_e \rangle + \langle Q_{o1} v_e N_e \rangle \right) \tag{13}$$

If one substitutes for j_i from equation (3), equation (13) becomes

$$\frac{1}{4} v_i N_i = \lambda N_o \left(\langle Q_{o1} v_e N_e \rangle + \langle Q_{o1} v_e N_e \rangle \right) \tag{14}$$

The thickness of the ionization region λ must be determined. Herein, we assume that this thickness is equal to the electron mean free path for collisions which result in the excitation of a ground state atom to the first excited state. The mean free path for ionization of these excited-state atoms is shorter than that for excitation, so that ionization from the excited state can readily occur in this ionization region. The mean free path for ground state ionization is larger than for excitation, but for the sheath voltage range considered herein (less than twice the ionization potential) this process is less likely than excitation. At higher voltages, however, one should use a different length to determine the ionization region thickness. Thus, in this study, we take λ to be

$$\lambda = \frac{\langle v_e N_e \rangle}{\langle Q_{o1} v_e N_e \rangle N_o} \tag{15}$$

With this definition of λ and using equations (12) and (14), equation (7) may be written as

$$p = \frac{\frac{1}{4} v_i N_o}{\langle v_e N_e \rangle} \left(\frac{\langle Q_{1i} v_e N_e \rangle + \langle Q_{o1} v_e N_e \rangle}{\langle Q_{oi} v_e N_e \rangle + \langle Q_{o1} v_e N_e \rangle} \right) \left(\frac{\langle Q_{o1} v_e N_e \rangle}{\langle Q_{1i} v_e N_e \rangle} \right) \tag{16}$$

In order to evaluate the term p, the electron distribution function must be known. It is quite likely that the electrons will be maxwellized (ref. 8) at some temperature less than the sheath voltage. We have used Dugan and Sovie results for electron temperatures from 1 to 25 volts and have found that the product of the terms multiplying the current ratio in equation (16) is less than 1. Therefore, if the electron current is large compared to the thermal flux of ground state atoms and if the temperature ratio r is large compared to 1, then p can be neglected. This implies that the degree of ionization in the ionization region is greater than 30 percent. Assuming this to be the case, equation (13) becomes

$$\frac{N_i}{N} = \frac{1}{1 + r} \tag{17}$$

Next, the electron temperature in the ionization region must be determined. We assume that the average energy of the electrons is less than the energy required for ionization from the first excited state, since this is the inelastic collision with the smallest energy transfer from the electron to the atom and, hence, the smallest mean free path. One may assume that the distribution of electrons with energy less than this energy $(\varphi_i - \varphi_1)$ will be such that the average energy will be one-half of this energy. That is, the electron temperature in the ionization region is

$$\frac{3}{2} kT_e = \frac{1}{2} e(\varphi_i - \varphi_1) \tag{18}$$

Therefore, the ratio of temperatures can be written as

$$r = \frac{T_e}{T} = \frac{e(\varphi_i - \varphi_1)}{3kT}$$

Bade and Yos perform the calculations in their model with $r = 1$. The above choice of r is the main difference between the present model and that of Bade and Yos.

Energy conservation. - An energy balance in the ionization region is

$$j_e V_{sh} = j_i \varphi_i + (j_e + j_i)\left(\frac{\varphi_i - \varphi_1}{2}\right) \tag{19}$$

where all of the ionization energy is assumed to return to the cathode, and the electrons leaving the ionization region carry the average energy into the discharge volume. The ratio of ion to electron current can be written as

$$\frac{j_i}{j_e} \equiv \gamma_i = \frac{V_{sh} - \frac{1}{2}(\varphi_i - \varphi_1)}{\varphi_i + \frac{1}{2}(\varphi_i - \varphi_1)} \tag{20}$$

The cathode spot energy equation (1) can be written using equation (19) as

$$4K(T_s - T_\infty) = \pi R\left\{(j_i + j_e)\left[V_{sh} - \varphi_w - \frac{1}{2}(\varphi_i - \varphi_1)\right] - \epsilon\sigma\left(T_s^4 - T_\infty^4\right)\right\} \tag{21}$$

If radiation is negligible (i.e., when the term involving the fourth power of temperature is small compared to the other terms in brackets), one can introduce

$$I = \pi R^2 (j_e + j_i) \tag{22}$$

and rewrite equation (21) as

$$4K(T_s - T_\infty) = \pi \sqrt{\frac{I}{\pi(j_e + j_i)}}\,(j_e + j_i)\left\{V_{sh} - \varphi_w - \frac{1}{2}(\varphi_i - \varphi_1)\right\} \tag{23}$$

Introduce the Richardson equation (eq. (2)) and γ_i from equation (20)

$$4K(T_s - T_\infty) = \sqrt{\pi I A_{rich}}\, T_s^2 \exp -\left\{\frac{e\varphi_w}{2kT_s}\right\}\sqrt{1 + \gamma_i}\left\{V_{sh} - \varphi_w - \frac{1}{2}(\varphi_i - \varphi_1)\right\} \tag{24}$$

A function Φ can be defined which does not depend upon the electrode temperature as

$$\Phi = \sqrt{1 + \frac{V_{sh} - \frac{1}{2}(\varphi_i - \varphi_1)}{\varphi_i + \frac{1}{2}(\varphi_i - \varphi_1)} \left\{ \frac{(V_{sh} - \varphi_w)}{\varphi_i} - \frac{1}{2} \frac{(\varphi_i - \varphi_1)}{\varphi_i} \right\}} \tag{25}$$

Defining

$$\left.\begin{aligned} I_{ref} &\equiv \frac{16\,K^2}{\pi A_{rich} \varphi_i^2} \\ \theta &\equiv \frac{kT_s}{e\varphi_w} \\ \theta_\infty &\equiv \frac{kT_\infty}{e\varphi_w} \end{aligned}\right\} \tag{26}$$

and

Equation (24) can then be written as

$$\sqrt{\frac{I}{I_{ref}}} = \frac{\theta - \theta_\infty}{\Phi} \frac{1}{\theta} \exp \frac{1}{2\theta} \tag{27}$$

This gives the current as a function of the spot temperature and the sheath voltage. Another relation between sheath voltage and temperature is determined by a combination of equations (3), (17), and (20):

$$\frac{V_{sh} - \frac{1}{2}(\varphi_i - \varphi_1)}{\varphi_i + \frac{1}{2}(\varphi_i - \varphi_1)} A_{rich} T_s^2 \exp - \left\{ \frac{e\varphi_w}{kT_s} \right\} = \frac{v_i}{4} \frac{N}{1 + r} \tag{28}$$

The ion current can be written in terms of the gas pressure and temperature as

$$j_{i,\max} = \frac{eNv_i}{4} = \frac{eP}{\sqrt{2kT\ \pi m_i}} = \frac{eP\sqrt{r}}{\sqrt{2kT_e\ \pi m_i}} \tag{29}$$

Equation (28) can then be written as

$$\left(\frac{e\varphi_w}{k}\right)^2 \frac{A_{rich}}{e} \frac{V_{sh} - \frac{1}{2}(\varphi_i - \varphi_1)}{\varphi_i + \frac{1}{2}(\varphi_i - \varphi_1)} \frac{1+r}{\sqrt{r}} \frac{\sqrt{2kT_e\ \pi m_i}}{P} = \frac{1}{\theta^2} \exp\frac{1}{\theta} \tag{30}$$

Define a reference pressure as

$$P_{ref} = \left(\frac{e\varphi_w}{k}\right)^2 \frac{A_{rich}}{e} \sqrt{\frac{2}{3}\pi m_i(\varphi_i - \varphi_1)e}$$

For argon and a cathode work function of 3.0 eV, $P_{ref} = 2.824\times10^{12}$ N/m^2. Then, if one defines a function Ψ as

$$\Psi \equiv \sqrt{\frac{1+r}{\sqrt{r}} \cdot \frac{P_{ref}}{P} \frac{V_{sh} - \frac{1}{2}(\varphi_i - \varphi_1)}{\varphi_i + \frac{1}{2}(\varphi_i - \varphi_1)}} \tag{31}$$

equation (30) becomes

$$\Psi = \frac{1}{\theta} \exp\frac{1}{2\theta} \tag{32}$$

This provides a relation between the gas properties, the work function, and the spot temperature. The function Ψ is plotted in figure 2.

To use this model one needs to specify only the gas, its pressure and temperature, the electrode work function, and undisturbed cathode temperature (away from the spot) in order to calculate the current-voltage characteristics. The radius of the spot, the heat transferred to the spot, and the current density can also be calculated.

The radius of the spot is

$$R = \sqrt{\frac{I}{\pi(j_e + j_i)}} \tag{33}$$

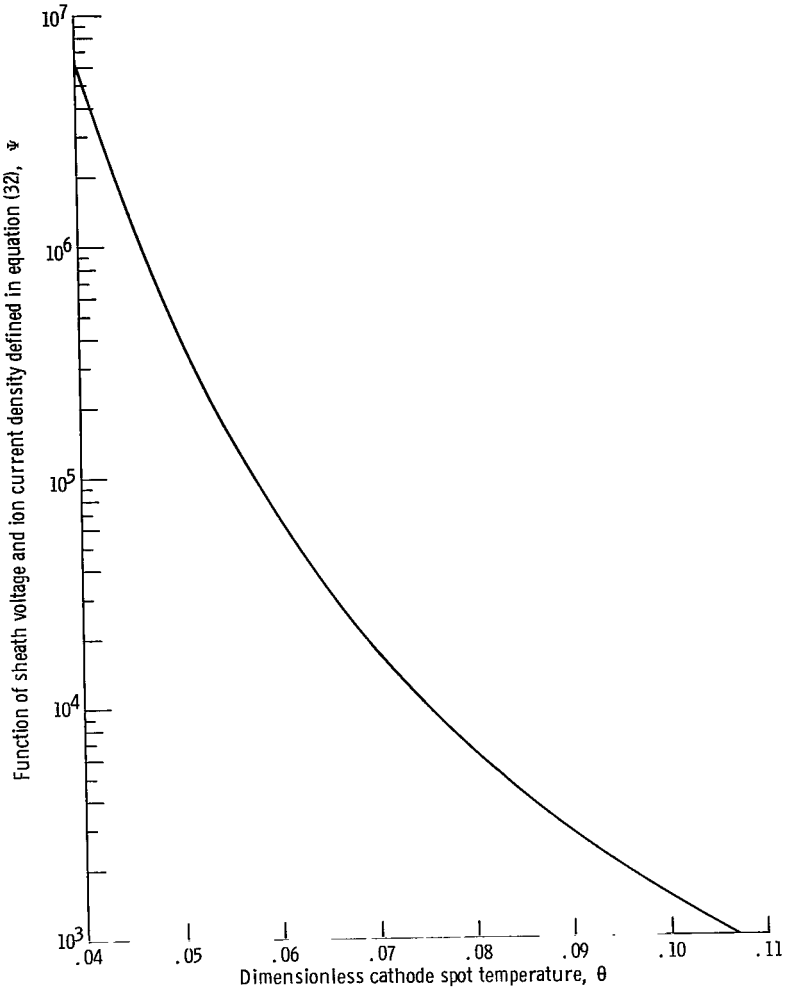

Figure 2. - Function of cathode sheath voltage and ion current density defined in equation (32) plotted as function of dimensionless cathode spot temperature.

This can be rewritten using equations (2), (20), and (26) to read

$$\frac{R}{R_{ref}} = \sqrt{\frac{I}{I_{ref}}} \left(\frac{1}{\theta} \exp \frac{1}{2\theta} \right) \frac{\varphi_i}{\varphi_w} \frac{1}{\sqrt{1 + \gamma_i}} \tag{34}$$

where

$$R_{ref} = \frac{4kK}{\pi A_{rich}\, e\, \varphi_i^2} \tag{35}$$

The heat transferred to the spot is

$$Q = 4RK(T_s - T_\infty) \tag{36}$$

which can be rewritten with the aid of equations (27) and (34) to read

$$\frac{Q}{Q_{ref}} = 4\left(\frac{I}{I_{ref}}\right)\frac{\Phi}{\sqrt{1 + \gamma_i}} \tag{37}$$

where

$$Q_{ref} = R_{ref}K\frac{e\varphi_i}{k} \tag{38}$$

The current density can be determined from equations (2) and (20)

$$j = j_e + j_i = A_{rich}T_s^2\left[\exp - \left(\frac{e\varphi_w}{kT_s}\right)\right](1 + \gamma_i) \tag{39}$$

which can be rewritten using equation (32) to read

$$\frac{j}{j_{ref}} = (1 + \gamma_i)\frac{1}{\Psi^2} \tag{40}$$

where

$$j_{ref} = A_{rich}\left(\frac{e\varphi_w}{k}\right)^2 \tag{41}$$

These parameters, along with the sheath voltage and spot temperature from equations (27) and (32) are shown in figures 3 to 5 for a work function of 3.0 eV. In each figure these parameters are shown for two ion temperatures, 500 and 1000 K, and for $P_{ref} = 2.824\times10^{12}$ newtons per square meter. In figure 3 the current is varied; in figure 4, the cathode temperature; and in figure 5, the pressure. As the current increases the sheath voltage decreases, and the other four quantities increase as can be seen in figure 3. The heat transfer increases rapidly with increasing current.

The sheath voltage and heat transfer decrease with increasing temperature; the

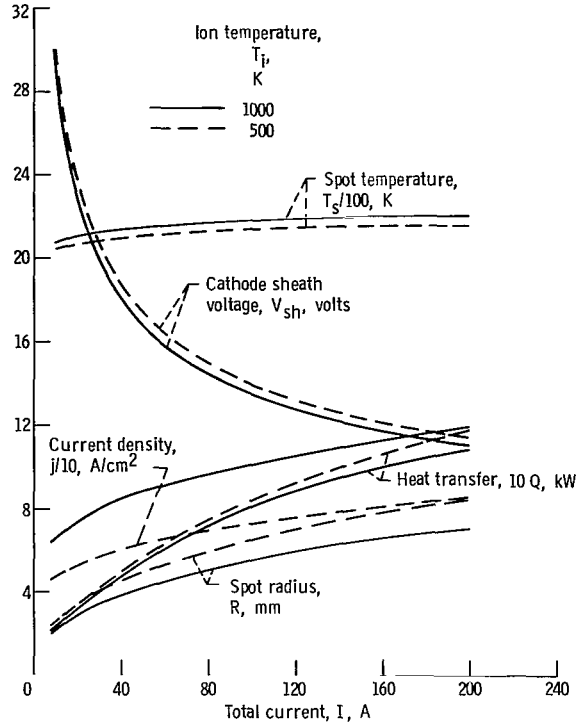

Figure 3. - Cathode spot parameters as function of current. Work function, 3.0 electron volts; pressure, 3.5x10^3 newtons per square meter; undisturbed cathode temperature, 1800 K.

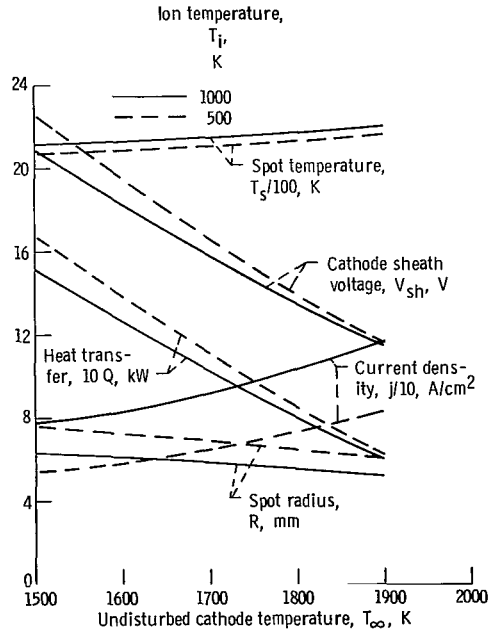

Figure 4. - Cathode spot parameters as function of undisturbed cathode temperature. Work function, 3.0 electron volts; pressure, 3.5x10^3 newtons per square meter; current, 100 amperes.

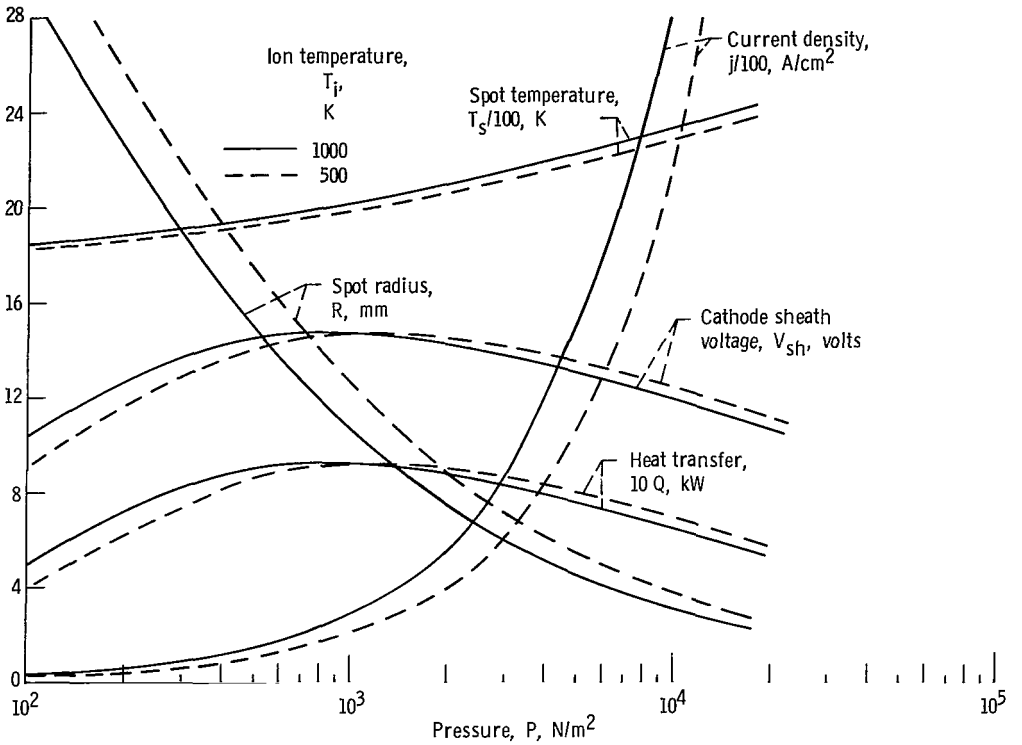

Figure 5. - Cathode spot parameters as function of pressure. Work function, 3.0 electron volts; current, 100 amperes; undisturbed cathode temperature, 1800 K.

other three quantities increase as can be seen in figure 4. The heat transfer is rather sensitive to the temperature.

In figure 5 it can be seen that the current density increases very rapidly with increasing pressure while the spot radius decreases and the spot temperature increases. The sheath voltage and heat transfer pass through a maximum value as the pressure increases. The low pressure region is characterized by a big spot and rather low temperature. The high pressure region is characterized by a small spot and high temperature.

EXPERIMENTAL APPARATUS AND MEASUREMENTS

Experiments conducted in a nonequilibrium argon plasma MHD generator led to the development of the physical model to explain the cathode spots. The experiment consisted of studying applied or magnetically induced voltages across a pair of plane-parallel electrodes immersed into hot-flowing argon. The electrodes were immersed to raise their temperature (T_∞ in the preceeding analysis) to provide thermionic emission.

Description of Apparatus

Arc heater and nozzle. - The arc heater is vortex stabilized and consists of a $1\frac{1}{8}$-inch-(32-mm-) diameter, annular, water-cooled copper anode and a water-cooled thoriated tungsten cathode. The argon flows into the arc through tangential holes.

A water-cooled convergent-divergent copper nozzle with a throat diameter of 1.44 inches (3.65 cm) and an area ratio of 4.34 is used. The Mach number at the nozzle exit, calculated for isentropic expansion of a perfect gas, is 3.6.

Test section. - The test section is a 7.6-centimeter-inside-diameter stainless steel tube 35.6 centimeters long. Thoriated tungsten (2 percent ThO_2) plate electrodes (0.76 mm × 1.27 cm × 2.22 cm) with pure tungsten stems are placed into the stream. To measure electrode drop and the voltage distribution across the electrode gap, nine pure tungsten wire probes (0.76 mm diam), insulated electrically from the test section, are placed on both sides of the test section in the direction of the B field and in the plane of the current path. They are spaced equally in a 3.8-centimeter electrode gap as shown in figure 6.

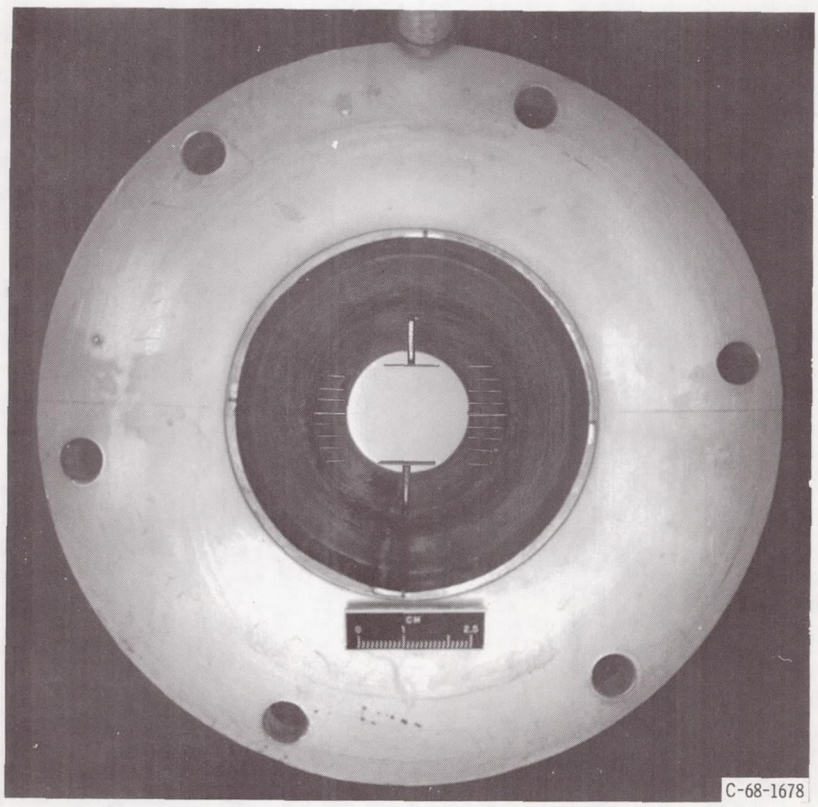

Figure 6. - End view of test section showing electrodes and voltage probes.

Experimental Measurements

Argon conditions. - The argon stagnation temperature was calculated calorimetrically. (Power into the gas is equal to the power into the arc minus the power into arc cooling water.) The static temperature was determined by assuming an isentropic expansion. The pressure was measured with a manometer.

Sheath voltage. - Cathode sheath voltage measurements were made for voltages applied across the electrodes and for voltages induced by flow through a magnetic field (i.e., MHD generator). The 80-volt dc power supply used for the applied voltage is limited to 50 amperes. The induced voltage is produced by a magnet with maximum magnetic field strength of 0.58 tesla. A typical set of voltage measurements is shown in figure 7. The cathode sheath voltage drop was the same for the two voltage sources.

Cathode spot temperature. - Electrode temperatures were measured by a two-color (wavelengths of 650 and 550 nm) pyrometer. The temperature is indicated on a meter calibrated in degrees with a linear scale. Also a millivolt output is used to record the data.

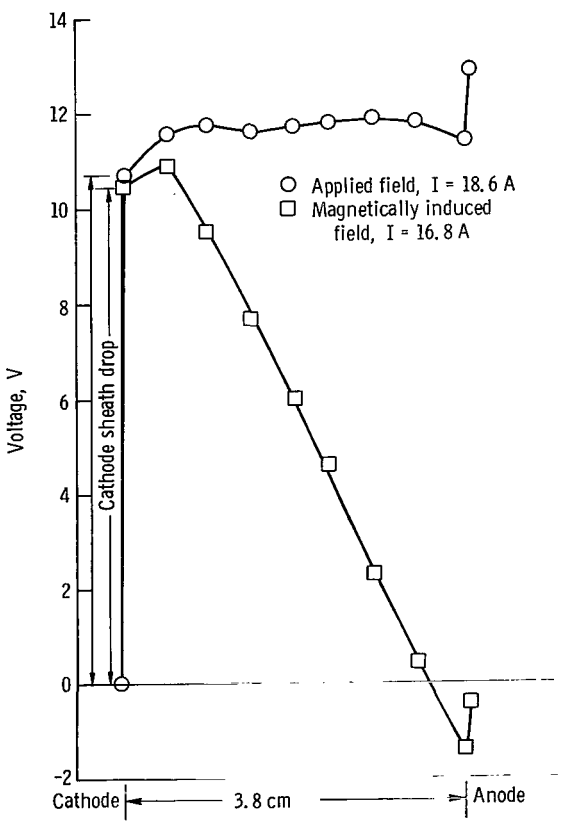

Figure 7. - Typical potential distribution across discharge.

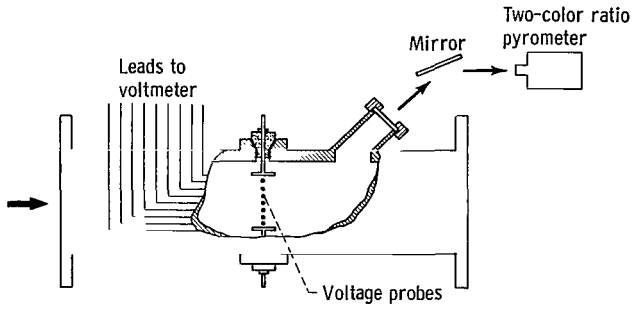

(a) Test section with voltage probes and pyrometer viewing port.

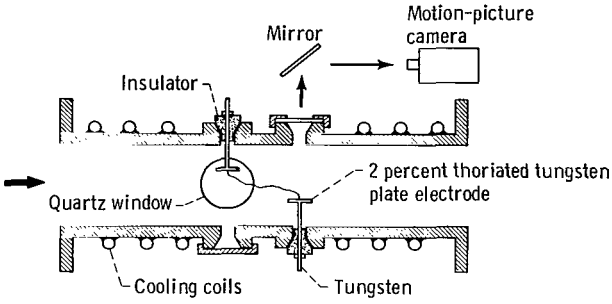

(b) Picture taking and spectrometer study section.

Figure 8. - Test sections.

The optical path for the pyrometer measurements included a quartz window and a mirror. Compared to a known temperature light source, this path introduced about a 1 percent error in the temperature measurement. It was found that during a run the quartz window did not discolor or lose its transparency. A cutaway sketch showing the pyrometer view and electrodes is shown in figure 8(a).

Photographs. - Color movies (24 f/sec, f 22, 90 ND, Ektachrome 16 mm) were taken of the cathode spot. The current-voltage and electrode temperature data were recorded at the same time so that current, arc spot size and temperature could be correlated. A sketch showing the camera and electrodes is shown in figure 8(b). Enlargements of typical frames are shown in figure 9.

Spectrographic study. - Spectrometer measurements were made for us by R. J. Sovie using a 1/2-meter Ebert monochrometer. A movable slit attached to a light-pipe scanned the gap between the electrodes. The lines examined were 434.8 nanometers (ion line) and 427.2 nanometers (neutral line). The ion line appears at the cathode but not at the anode. This is shown in figure 10. The neutral line studied at the same time indicated a relatively uniform distribution in the electrode gap.

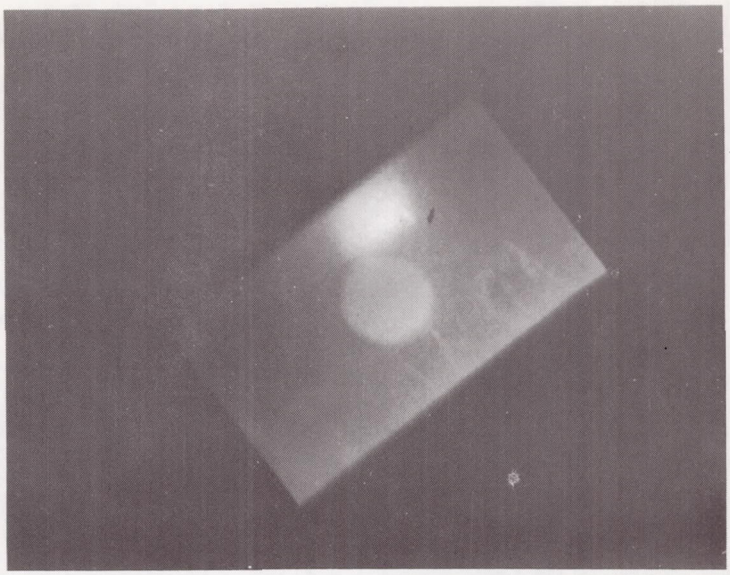

(a) Magnetic field applied, 20 amp.

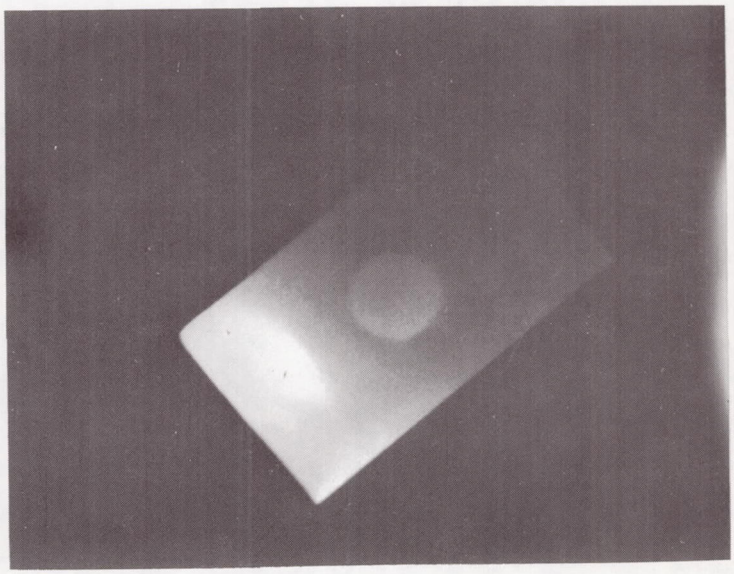

(b) No magnetic field, 40 amp.

Figure 9. - Photographs of arc spots. Electroce size is 1.27x2.22 cm. Circles in center are support rod welds.

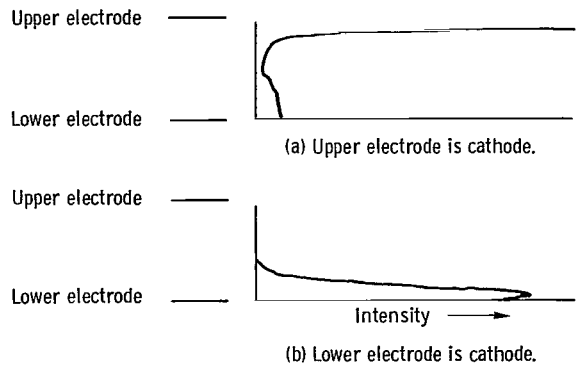

Figure 10. - Argon ion line (434.8 nm) intensity profile for discharge current of 30 amperes. Distance between electrodes, 1.27 centimeters.

RESULTS AND DISCUSSION

Comparison of Model and Experiment

Presence of cathode spot and ionization region. - The sample photographs (movie frames) of cathode spots shown in figure 9 were for two currents. Note that the spot becomes brighter and larger at the higher current. (The bright circle in the center of the electrode is the support rod weld.)

From the ion line intensity profiles (shown in fig. 10), it is apparent that there is a region with large ion number density near the cathode, regardless of whether it is the upper or lower electrode. This region is identified with the ionization region of the model used in the analysis.

Sheath voltage and cathode spot temperature. - Equation (32) provides a relation between the spot temperature and the sheath voltage. Three parameters must be specified:

TABLE I. - EXPERIMENTAL CONDITIONS IN TEST SECTION

Run	Pressure, P, N/cm^2	Ion temperature, T_i, K	Work function, φ_w, eV	Undisturbed cathode temperature, T_∞, K	Maximum ion current density, $j_{i,max}$, A/cm^2
1	0.234	990	3.25 to 3.35	2080	499
2	.298	540	2.7	1780	858
3	.234	1025	3.2 to 3.6	2080	489

the argon pressure, argon temperature, and the work functions. These parameters are shown in table I for three experimental runs. The resulting theoretical values are compared with the experimental data in figure 11. The work function shown in table I was determined as the value which gave the best fit to the experimental data. Further discussion on this point is found in the section entitled Work function.

The curves seem to fit the data except when the sheath voltage is below 14 volts, which is near the excitation potential (11.4 V). It is likely that the model describing the

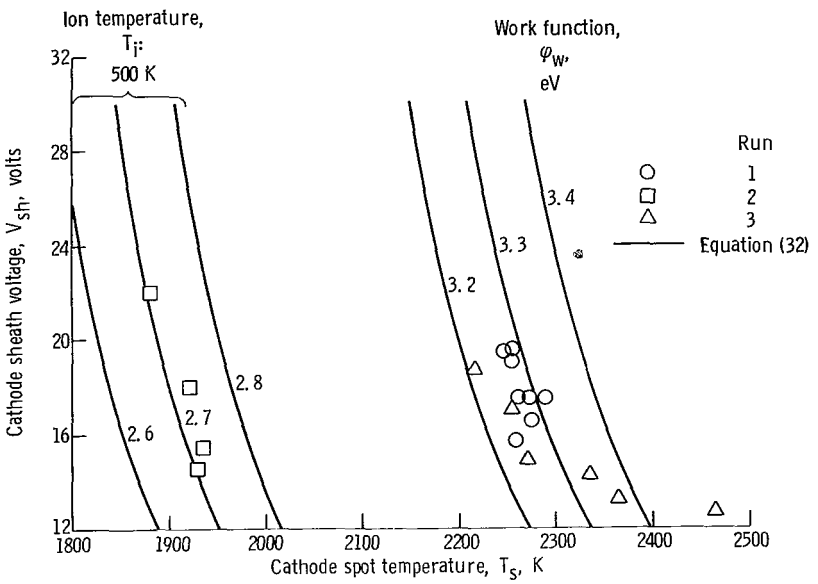

Figure 11. - Cathode sheath voltage as function of cathode spot temperature at two ion temperatures and three different values of work function at each ion temperature.

processes in the ionization region is inaccurate for voltages near the excitation potential. Also, the spot radius becomes larger at high spot temperature and may not be small compared to the cathode dimensions.

Current-voltage characteristics. - Using the parameters in table I, the current-voltage characteristics were calculated from equation (27), with θ determined from equation (32). In figure 12 these characteristics are compared with the experimental data. A reasonable agreement is noted, giving added confidence to the values of work function selected from figure 11.

Spot radius and spot temperature. - The spot radius as a function of spot temperature

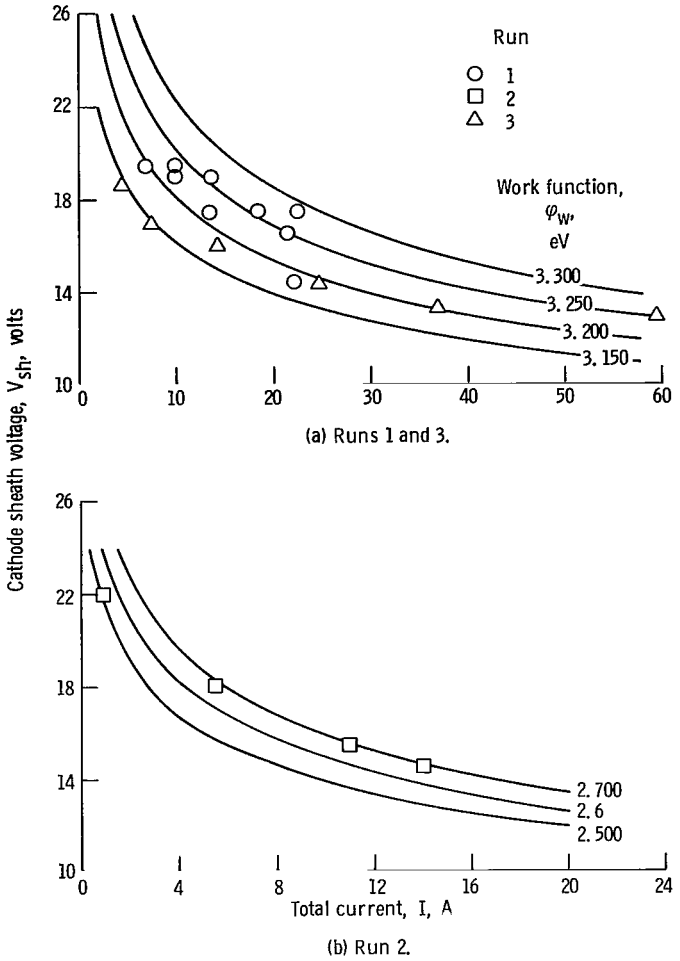

Figure 12. - Cathode sheath voltage as function of total current in argon for different values of cathode work function.

calculated from equation (34) is compared in figure 13 with values measured from photographs similar to those in figure 9. The radius is defined as

$$R = \sqrt{\frac{A}{\pi}} \tag{42}$$

where the area is measured by using a planimeter. The agreement is again reasonable for the work functions determined from figure 11. Further evidence of agreement from the same experiment is the fact that the radius is quite sensitive to changes in spot temperature and work function.

Work function. - The work function obtained from the best fit of the sheath voltage as a function of cathode spot temperature data (fig. 11) is plotted as a function of spot

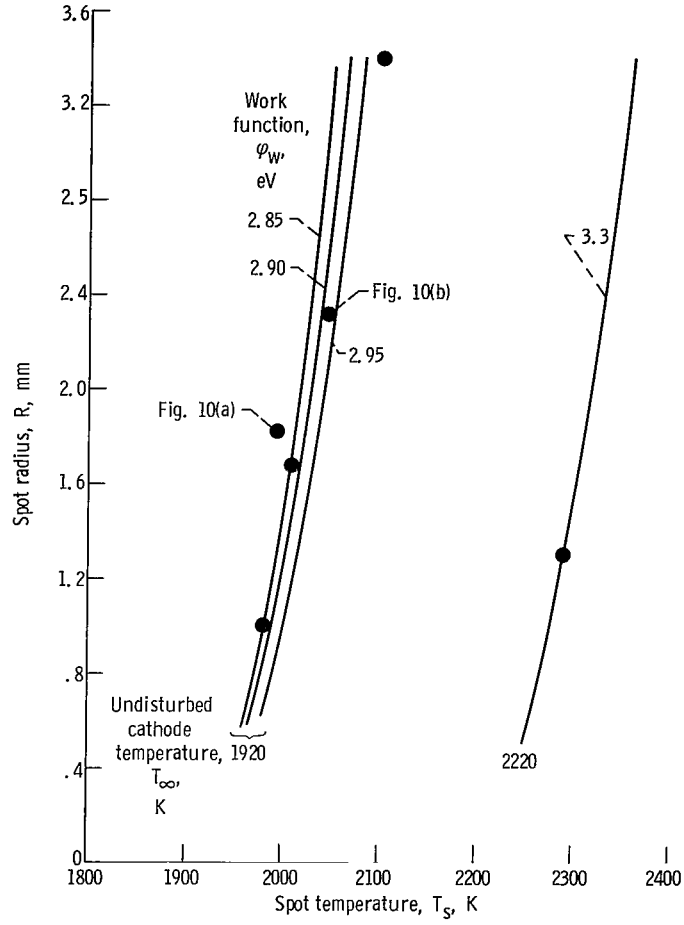

Figure 13. - Cathode spot radius as function of spot temperatures at two different undisturbed cathode temperatures.

temperature in figure 14. Also in figure 14 the work function is obtained from figure 13. The agreement between the two methods is reasonably good. The data used in the two methods was taken on different runs.

From figure 14, the work function for the unactivated cathodes used in the experiment is 2.7. The Richardson equation constant in our calculations is set equal to 1.2×10^6 amp/$(m^2)(K^2)$. However, other experimentors (e.g., ref. 11) have found work functions for activated thoriated tungsten in vacuum to be 2.6 eV and A_{rich} equal to 3×10^4 amp/$(m^2)(K^2)$ or 3.2 eV using our assumed A_{rich} of 1.2×10^6 amp/$(m^2)(K^2)$ at 1900 K.

The difference of about 0.5 eV in the work function mentioned above may be explained by the difference in cathode preparation (activation process) and cathode operating conditions.

During the activation process (electrodes being heated to a high temperature in our case) oxides are reduced. The presence of oxygen on the cathode may explain our lower

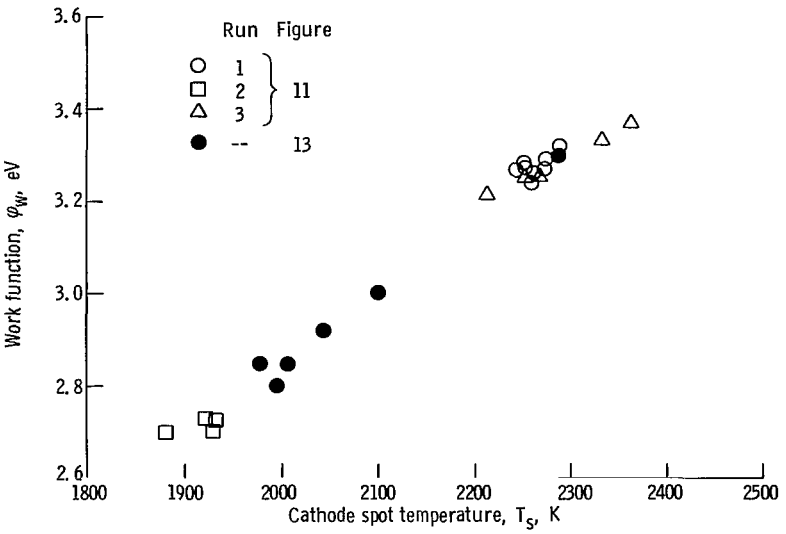

Figure 14. - Work function determined from figures 11 and 13 as function of cathode spot temperature.

work function once emission has been obtained. Many investigators have noted that both for tungsten cathodes in the presence of cesium and barium (ref. 10, pp. 56-58) and for copper electrodes in the presence of cesium (ref. 12) emission is improved (i.e., the work function is lowered) in the presence of oxygen. Since "the mechanism of the emission of the tungsten-thorium cathode is exactly the same as that of tungsten-cesium and the tungsten-barium cathodes." (ref. 11, p. 55), it seems likely that oxygen has also lowered the work function of the unactivated thoriated tungsten electrodes tested herein, as well as permitting higher operating temperatures. It can also be seen from figure 14 that at 2300 K the work function of our unactivated cathodes has increased to 3.3 eV, indicating that the active material is being removed and that the work function is approaching that of pure tungsten, 4.5 eV.

Further evidence that the presence of oxygen lowered the work function of the cathodes was gathered by carbonizing (as described in ref. 13) some cathodes and studying them. The work function at 2150 K increased from 3.1 for the uncarbonized cathode to 3.5 eV for the carbonized cathode. Also, no spots were observed. The work function for lower cathode temperatures (i.e., without a spot) was probably lowered by the activation process. However, at higher temperatures (i.e., with a spot when using unactivated cathodes) the presence of oxygen for the unactivated cathode then provided the lower work function described previously. This explanation is consistent with the observations of Hermann and Wagner who state "that the work function of atomic film cathodes such as W-Ba, W-Ca, etc. can be both decreased and increased by the absorption of oxygen, and that the position of oxygen relative to the other absorbed material is decisive." (ref. 11, p. 58).

Comparison with Previous Models

The present model incorporates the properties of the cathode and the plasma in such a way that the cathode spot parameters can be deduced with no emperical constants required. Therefore, the results from this model can be compared directly only with those of the Bade and Yos model. For the experimental conditions considered herein, the Bade and Yos model gives sheath voltages about 4 volts lower, current density about twice as large, a radius about 2/3 as large, heat transfer to the cathode about 30 percent less, and a spot temperature about 100° higher than the present model. The present model is an improvement of the Bade and Yos model without an undue increase in complexity since it has been shown that the present model agrees fairly well with the experiment.

Implication for Generator Design

It is desirable to maintain a low heat transfer to the cathode of an MHD generator. This is an energy loss and contributes to reducing the efficiency. In order to maintain a low heat transfer to the cathode the undisturbed cathode temperature should be kept high. These high temperatures also reduce the sheath voltage drop at the cathode, which is important in providing generators with high isentropic efficiency.

The heat transfer also decreased with increasing pressure. However, the spot temperature became high and spot size became small. This may lead to a reduced cathode life because of erosion and depletion of thoria.

CONCLUDING REMARKS

The simple model used in this study agrees quite well with some experimental data for electrode phenomena. The results are qualitatively the same as that of Bade and Yos, but agreement with our experiment is improved. A major conclusion is that higher temperature electrodes will decrease the sheath voltage and, hence, the heat transfer losses to the cathode. This conclusion is important in determining the performance of MHD generators.

Lewis Research Center,
National Aeronautics and Space Administration,
Cleveland, Ohio, May 23, 1969,
129-02-08-05-22.

APPENDIX - SYMBOLS

A_{rich}	Richardson's constant, 1.2×10^{6} A/(m^2)(K^2)
e	electrical charge, 1.6×10^{-19} C
I	current
j	current density
K	thermal conductivity
k	Boltzman constant, 1.38×10^{-23} J/K
m	particle mass
N	number density
P	pressure
p	parameter defined in eq. (15)
Q	heat transfer
R	spot radius
r	ratio of electron to ion temperature
T	temperature
V	voltage
v_i	velocity
ϵ	emissivity
θ	nondimensional temperature
λ	thickness of ionization region
σ	Stefan-Boltzmann constant, 5.75×10^{-12} W/(cm^2)(K^4)
Φ	parameter defined in eq. (25)
φ	potential (ionization, excitation); or work function
Ψ	parameter defined in eq. (29)

Subscripts:

e	electron
i	ion
o	neutral
ref	reference
s	spot
sh	sheath
w	work function
1	excited state
∞	at a large distance from spot

REFERENCES

1. Somerville, J. M.: The Electric Arc, Methuen and Co., Ltd., 1959, pp. 64-68.
2. Ecker, G.: Die Stabilisierung des Lichtbogens for Anode und Kathode, Z. Physik 136, 1-16 (1953).
3. Bauer, A.: Untersuchungen uber den Kathodenfall in den Ubergangsbereichen vom Thermobogen zum Feldbogen und vom Bogen zur Glimmentladung, Ann. Physik 18, pp. 387-400, 1956.
4. Lee, T. H.; and Greenwood, A.: Theory for the Cathode Mechanism in Metal Vapor Arcs, J. of App. Phys., Vol. 32, No. 5, May 1961, pp. 916-923.
5. Adams, R. C.; and Robinson, E.: Electrode Processes in MHD Generators, Proc. of IEEE, Vol. 56, No 9, Sept. 1968, pp. 1519-1535.
6. Bade, W.; and Yos, J.: Theoretical and Experimental Investigation of Arc Plasma-Generation and Technology, PAT II: Applied Research on Electric Arc Phenomena, Vol. 1: A Theoretical and Experimental Study of Thermionic Arc Cathodes. ASD-TDR-62-729 (Contract No. AF33(616)-7578), Avco Corporation, Wilmington, Mass., Sept. 1963.
7. Dugan, J. V., Jr.: The Selection of Simple Model Atoms for Calculation of Electron Density in Non-Equilibrium, Low Temperature Cs Plasmas, 27th Annual Conference Physical Electronics, Mar. 20-23, 1967, MIT, pp. 323-331. (Also, NASA TM X-52291.)
8. Dugan, J. V., Jr.; and Sovie, R. J.: Volume Ion Production Costs in Tenuous Plasmas, NASA TN D-4150.
9. Grober, H.; Erk, S.; and Grigull, V.: Fundamentals of Heat Transfer, Third Edition, McGraw-Hill, 1961, pp. 115-119.
10. Stankiewicz, N.: Limits of Validity of Radiationless Decay of High-Density Plasmas. NASA TN D-3372, June 1966.
11. Hermann, G.; and Wagner, Phil. S.: The Oxide Coated Cathode, Chapman & Hall, London, Volz.
12. Wilson, R. G.: Electron and Ion Emission From a Copper Surface in the Presence of Oxygen, Cesium, and Oxygen plus Cesium, Surface Science. Vol. 7, June 1967, pp. 157-174.
13. Schneider, P.: Thermionic Emission of Thoriated Tungsten. Journal of Chemical Physics, Vol. 28, No. 4, April 1958, p. 677.

NASA-Langley, 1969 —— 25 E-5100

NATIONAL AERONAUTICS AND SPACE ADMINISTRATION
WASHINGTON, D.C. 20546

OFFICIAL BUSINESS

FIRST CLASS MAIL

POSTAGE AND FEES PAID
NATIONAL AERONAUTICS AN
SPACE ADMINISTRATION

"The aeronautical and space activities of the United States shall be conducted so as to contribute . . . to the expansion of human knowledge of phenomena in the atmosphere and space. The Administration shall provide for the widest practicable and appropriate dissemination of information concerning its activities and the results thereof."

—NATIONAL AERONAUTICS AND SPACE ACT OF 1958

NASA SCIENTIFIC AND TECHNICAL PUBLICATIONS

TECHNICAL REPORTS: Scientific and technical information considered important, complete, and a lasting contribution to existing knowledge.

TECHNICAL NOTES: Information less broad in scope but nevertheless of importance as a contribution to existing knowledge.

TECHNICAL MEMORANDUMS: Information receiving limited distribution because of preliminary data, security classification, or other reasons.

CONTRACTOR REPORTS: Scientific and technical information generated under a NASA contract or grant and considered an important contribution to existing knowledge.

TECHNICAL TRANSLATIONS: Information published in a foreign language considered to merit NASA distribution in English.

SPECIAL PUBLICATIONS: Information derived from or of value to NASA activities. Publications include conference proceedings, monographs, data compilations, handbooks, sourcebooks, and special bibliographies.

TECHNOLOGY UTILIZATION PUBLICATIONS: Information on technology used by NASA that may be of particular interest in commercial and other non-aerospace applications. Publications include Tech Briefs, Technology Utilization Reports and Notes, and Technology Surveys.

Details on the availability of these publications may be obtained from:

SCIENTIFIC AND TECHNICAL INFORMATION DIVISION

NATIONAL AERONAUTICS AND SPACE ADMINISTRATION

Washington, D.C. 20546